

## Formation of Sn nanocrystals in thin SiO<sub>2</sub> film using low-energy ion implantation

Anri Nakajima, Toshiro Futatsugi, Naoto Horiguchi, and Naoki Yokoyama

Citation: *Applied Physics Letters* **71**, 3652 (1997); doi: 10.1063/1.120470

View online: <http://dx.doi.org/10.1063/1.120470>

View Table of Contents: <http://scitation.aip.org/content/aip/journal/apl/71/25?ver=pdfcov>

Published by the [AIP Publishing](#)

---

### Articles you may be interested in

[Charge trapping and retention behaviors of Ge nanocrystals distributed in the gate oxide near the gate synthesized by low-energy ion implantation](#)

*J. Appl. Phys.* **101**, 124313 (2007); 10.1063/1.2749470

[Effect of annealing environment on the memory properties of thin oxides with embedded Si nanocrystals obtained by low-energy ion-beam synthesis](#)

*Appl. Phys. Lett.* **83**, 168 (2003); 10.1063/1.1588378

[Microstructure and electrical properties of Sb nanocrystals formed in thin, thermally grown SiO<sub>2</sub> layers by low-energy ion implantation](#)

*J. Vac. Sci. Technol. B* **17**, 1317 (1999); 10.1116/1.590753

[Coulomb blockade in Sb nanocrystals formed in thin, thermally grown SiO<sub>2</sub> layers by low-energy ion implantation](#)

*Appl. Phys. Lett.* **73**, 1071 (1998); 10.1063/1.122087

[Microstructure and electrical properties of Sn nanocrystals in thin, thermally grown SiO<sub>2</sub> layers formed via low energy ion implantation](#)

*J. Appl. Phys.* **84**, 1316 (1998); 10.1063/1.368199

---

The advertisement features a 3D cutaway of a mechanical part with a rainbow-colored stress or temperature distribution. The text 'Over 600 Multiphysics Simulation Projects' is prominently displayed in white and blue. A blue button with white text says 'VIEW NOW >>'. The COMSOL logo is in the bottom right corner.

Over **600** Multiphysics  
Simulation Projects

[VIEW NOW >>](#)

COMSOL

# Formation of Sn nanocrystals in thin SiO<sub>2</sub> film using low-energy ion implantation

Anri Nakajima,<sup>a)</sup> Toshiro Futatsugi, Naoto Horiguchi, and Naoki Yokoyama  
*Fujitsu Laboratories Limited, 10-1 Morinosato-Wakamiya, Atsugi 243-01, Japan*

(Received 20 March 1997; accepted for publication 21 October 1997)

This letter reports on a simple technique for fabricating Sn nanocrystals in thin SiO<sub>2</sub> film using low-energy ion implantation followed by thermal annealing. These Sn nanocrystals have excellent size uniformity and position controllability. Their average diameter is 4.8 nm with a standard deviation of 1.0 nm. Most of the Sn nanocrystals reside at the same depth. The lateral edge-to-edge spacing between neighboring Sn nanocrystals is fairly constant: about 3 nm. A narrow as-implanted ion distribution profile and the effect of the SiO<sub>2</sub>-Si interface are considered to contribute to the size uniformity and position controllability. The features of these nanocrystals will open up new possibilities for novel devices. © 1997 American Institute of Physics. [S0003-6951(97)01451-4]

Metal nanocrystals are expected to exhibit unique physical properties due to the single electron effect<sup>1</sup> and their large nonlinear optical properties.<sup>2-4</sup> The possibility of using these structures not only for studying various aspects of physics but also for creating new devices is stimulating much research in this field. To create such devices, we need precise control over the size and position of the nanocrystals. Furthermore, the ideal technique would be compatible with conventional large-scale integration device fabrication methods. This way, we could use a proven, mature Si technique to further investigate the possibilities of new devices.

Metal or semiconductor nanocrystals in barrier materials with low dielectric constants have the advantage of exhibiting the single electron effect at high temperatures, since the total capacitance of the dots decreases in such materials. The advantage of using metal instead of semiconductor nanocrystals is that a large number of electrons can enter metal nanocrystals because the energy separation of the quantum levels in such nanocrystals is negligible. This negligible quantum-level separation also results in a constant addition energy. In addition, metal nanocrystals embedded in dielectric materials exhibit a large third-order susceptibility and a picosecond response time. Their structure is also favorable for applications to optical waveguides and other optical devices.<sup>2-4</sup>

Ion implantation is a promising fabrication technique for forming nanocrystals in dielectric materials. This technique can enable the controlled depth distribution of a desired species and is extensively used in semiconductor technology. To our knowledge, the formation of Cu,<sup>5</sup> Ag,<sup>6,7</sup> Au,<sup>4</sup> and Fe (Ref. 8) metal nanocrystals in implanted glass has so far been reported.

In this letter, we report on a fascinating method to fabricate metal nanocrystals in extremely thin SiO<sub>2</sub> layers by the low-energy ion implantation of Sn<sup>+</sup> ions followed by thermal annealing. With this method, we formed an array of Sn nanocrystals with excellent size uniformity and position controllability.

The low-energy implantation of Sn<sup>+</sup> ions was done at an energy of 10 keV and a dose of  $5 \times 10^{15}$  ions/cm<sup>2</sup> to a 15 nm thick SiO<sub>2</sub> layer thermally grown on a Si substrate. The Si

substrate was heavily doped with Sb. The calculated projected range was at the center of the SiO<sub>2</sub> layer, and the projected standard deviation was 2.0 nm. Subsequent thermal annealing was carried out in a N<sub>2</sub> ambient at 900 °C for 10 min.

We studied the size and position of Sn dots using transmission electron microscopy (TEM) with a Hitachi H-9000NAR operating at 300 kV. The chemical composition of the dots was determined with a field-emission analytical electron microscope operating at an acceleration voltage of 200 kV. An energy dispersive x-ray (EDX) spectrometer with a solid angle of 0.12 sr was attached to the microscope. The Sn dots were analyzed using an electron beam about 1 nm in diameter.

Figure 1 shows a cross-sectional TEM micrograph of nanoscale Sn dots in a thin SiO<sub>2</sub> layer formed by low-energy ion implantation. It is evident that spherical Sn dots with excellent size uniformity exist in the thin SiO<sub>2</sub> layer. The average diameter of 28 measured dots was 4.8 nm with a standard deviation of 1.0 nm. The Sn nanocrystals' position shifted slightly from the center of the thin SiO<sub>2</sub> layer to the SiO<sub>2</sub>-Si interface. Figure 2 is a high-resolution TEM micrograph of the Sn dots. Clear lattice images indicate that the Sn dots are indeed crystalline.

To confirm the chemical composition of these nanocrystals, we took EDX measurements (Fig. 3). In Fig. 3, the circles represent measurements on the core region of the nanocrystals, and the squares are those on a region far from the nanocrystals. The obvious Sn peaks at the core region

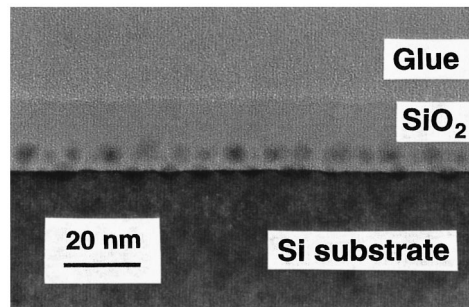


FIG. 1. Cross-sectional TEM micrograph of Sn nanocrystals in a thin SiO<sub>2</sub> layer fabricated using low-energy ion implantation.

<sup>a)</sup>Electronic mail: nakajima@qed.flab.fujitsu.co.jp

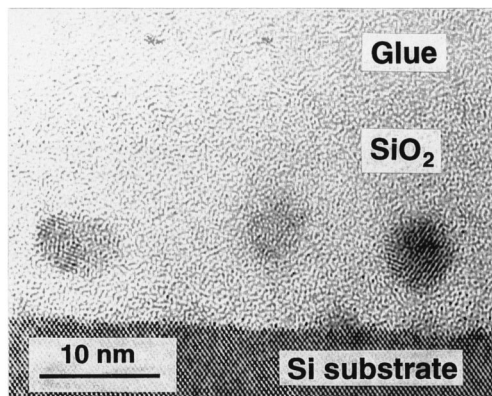


FIG. 2. High-resolution cross-sectional TEM micrograph of Sn nanocrystals in a thin SiO<sub>2</sub> layer fabricated using low-energy implantation.

reveal that the nanocrystals include Sn ions. The almost identical peak ratio of Si to O in both regions indicates that most of the oxygen combined with Si in both regions. This implies that hardly any oxygen combined with Sn ions and suggests that the formed nanocrystals are metal Sn.

To our knowledge, the size uniformity of such fabricated Sn nanocrystals is the best among those ever reported for metal nanocrystals. For example, Ag nanocrystals formed in glass using ion implantation with 60 keV at a dose of  $4 \times 10^{16}/\text{cm}^2$  have an average diameter of 4.2 nm with a standard deviation of 3.7 nm.<sup>7</sup> For further comparison purposes, we referred to the reported average diameter of 9.8 nm and the standard deviation of 3.4 nm for Si dots fabricated by electron-beam lithography and subsequent dry and wet etchings.<sup>9</sup> The standard deviation of the Sn dots fabricated in this study was better than that of such artificially fabricated Si dots. Furthermore, the technique we propose offers excellent control over dot positioning. Although we can observe the existence of nanoscale dots at the SiO<sub>2</sub>-Si interface in Figs. 1 and 2, most of the Sn nanocrystals in the SiO<sub>2</sub> layer reside at the same depth. In the lateral direction, the edge-to-edge spacing between neighboring Sn nanocrystals in the SiO<sub>2</sub> layer is also fairly constant: about 3 nm.

We used EDX line analysis to investigate the distribution of Sn ions after thermal annealing (Fig. 4). In this mea-

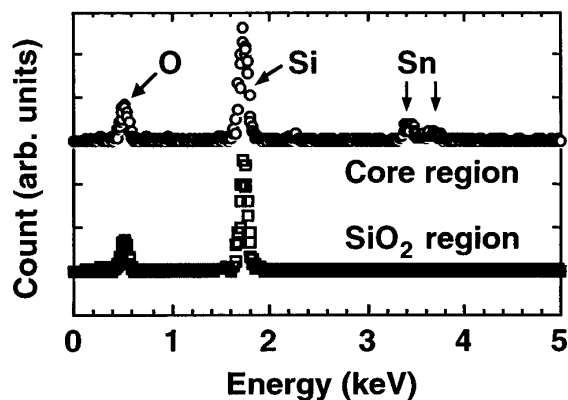


FIG. 3. EDX spectra from the core region of Sn dots (circles) and from a region far from the Sn dots (squares) in a thin SiO<sub>2</sub> layer.

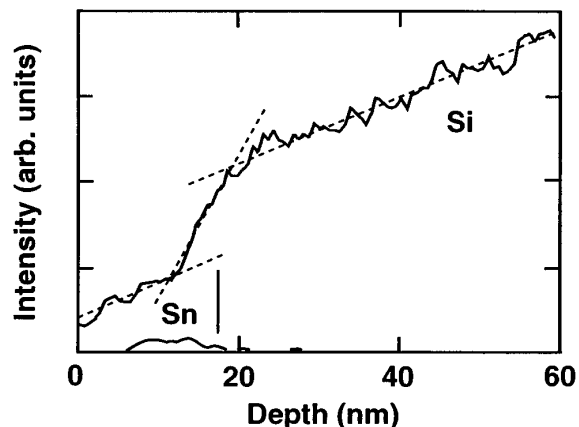


FIG. 4. EDX line analysis for a sample with Sn nanocrystals in a thin SiO<sub>2</sub> layer. An electron beam intersected both the Sn nanocrystal in the SiO<sub>2</sub> layer and that at the SiO<sub>2</sub>-Si interface. Si intensity was monitored as a reference. SiO<sub>2</sub>-Si interface position is shown by the bar.

surement, an electron beam scanned along the depth direction with the EDX intensity being monitored as a function of the depth position. The scanned line intersected both the Sn nanocrystal in the SiO<sub>2</sub> layer and that at the SiO<sub>2</sub>-Si interface. As a reference, the signal intensity of Si was also monitored. In Fig. 4, the position of the SiO<sub>2</sub>-Si interface is shown by the bar. The intensity of Si essentially increases with depth, as indicated by the broken lines. The slopes of this line for the SiO<sub>2</sub> region near the surface and that for the Si substrate region are almost the same. This increase of intensity is considered to correspond to the thickness of the sample, which increases with depth. In spite of this thickness increase with depth, the intensity of Sn is reduced to the noise level in the Si substrate region below about 2 nm from the SiO<sub>2</sub>-Si interface. This indicates that the Sn concentration in this region is almost negligible. On the contrary, in the SiO<sub>2</sub> layer, strong Sn peaks were observed in the region whose center depth had slightly shifted from the center of the SiO<sub>2</sub> layer to the interface. This is consistent with the position of Sn nanocrystals in Figs. 1 and 2. It should be noted that we can see a small but nevertheless existing Sn peak occurs around the SiO<sub>2</sub>-Si interface region. This indicates that a small amount of Sn exists at this interface region. However, this existing Sn region is limited to within about a 2 nm depth from the interface. Judging from the lattice image of the dots at the interface in the TEM micrographs of Figs. 1 and 2, Sn ions may have formed an alloy with Si at the interface of the Si substrate. For the above-mentioned reasons, we can safely say that an excellent depth control of Sn nanocrystals was achieved by our process.

It should be pointed out that the slope of the broken line for the SiO<sub>2</sub> layer near the SiO<sub>2</sub>-Si interface is larger than those of the other two regions. This indicates that the Si concentration in the SiO<sub>2</sub> layer near the interface, when normalized by the thickness of the sample, is larger than that in the SiO<sub>2</sub> layer near the surface and smaller than that in the Si substrate. This suggests the possible existence of a transition region where the bonding changes from SiO to SiO<sub>2</sub>. It is reported<sup>10</sup> that the thermal oxide is under compression due to

the density mismatch between Si and SiO<sub>2</sub> in the transition region.

To investigate the effect of the SiO<sub>2</sub>-Si interface on the size and position distribution of Sn nanocrystals, we took a cross-sectional TEM micrograph of a thick thermally grown SiO<sub>2</sub> sample (0.5 μm) that was Sn implanted and subsequently annealed. The Sn implantation and annealing conditions were the same as those for the thin SiO<sub>2</sub> sample. A trace of Sn dots can also be seen in the cross-sectional TEM micrograph for the thick SiO<sub>2</sub> sample. However, the size of the Sn dots was much smaller (a typical diameter of 2 nm) and they were dispersed more along the depth direction (from about 10 nm to 50 nm from the surface) when compared with those in the thin SiO<sub>2</sub> sample. This dispersion, in turn, indicates that the transfer of Sn ions from the SiO<sub>2</sub> layer to the Si substrate is suppressed in the thin SiO<sub>2</sub> sample.

Several possible reasons can account for this suppression. One is that the diffusion of Sn ions is much faster in SiO<sub>2</sub> than in Si. Another is that the segregation coefficient  $m$  of Sn is much smaller than unity, where  $m$  equals the impurity equilibrium concentration in Si divided by that in SiO<sub>2</sub>. A final reason is that the diffusion of Sn ions in the SiO<sub>2</sub> layer near the SiO<sub>2</sub>-Si interface is much slower due to the compressive strain in that region. Considering the gradual decrease of Sn concentration with depth in the SiO<sub>2</sub> layer near the interface (Fig. 4), this last reason is the most plausible since the former two reasons lead to an abrupt change of Sn concentration at the SiO<sub>2</sub>-Si interface.

Also, in the cross-sectional TEM micrograph for the thick SiO<sub>2</sub> sample, no trace of Sn dots is observed in the region from the surface to about 10 nm in depth. This suggests that Sn ions are depleted in this region. This Sn depletion is thought to be due to the escape of some Sn ions from the SiO<sub>2</sub> layer into ambient gas.

A number of comments can be made regarding the extremely narrow size and position distribution of Sn nanocrystals in the thin SiO<sub>2</sub> layer. It has been reported<sup>11</sup> that the diameter of Cu nanocrystals in SiO<sub>2</sub> glass increases linearly with the implanted Cu concentrations. Although subsequent thermal annealing was not carried out in that report, the results suggest the strong correlation between nanocrystal size and as-implanted ion concentration even when subsequent annealing has been done. For thin SiO<sub>2</sub> layers, a narrow as-implanted ion distribution can be achieved with low-energy ion implantation and maintained sufficiently during thermal annealing due to the slow diffusion of Sn ions in the SiO<sub>2</sub>

region near the SiO<sub>2</sub>-Si interface. This will lead to an excellent size and position uniformity of the formed Sn nanocrystals. The escape of Sn ions from the SiO<sub>2</sub> layer into the gaseous ambient may also occur in the thin SiO<sub>2</sub> sample. This lowers the Sn concentration near the surface of the SiO<sub>2</sub> and contributes to maintaining the narrow ion distribution during thermal annealing.

Another possible reason, which would lead to the size uniformity of Sn nanocrystals, is that the compressive strain that exists in the SiO<sub>2</sub> near the SiO<sub>2</sub>-Si interface due to the density mismatch may be reduced by the forming of Sn nanocrystals in that region. An appropriate nanocrystal size that minimizes the strain energy will then exist. This effect will also be closely related to the distribution of Sn nanocrystals. The lateral and depth positions of Sn nanocrystals will be those that minimize the strain energy.

In summary, we developed a simple technique for fabricating Sn nanocrystals in thin SiO<sub>2</sub> layers using low-energy ion implantation followed by thermal annealing. Sn nanocrystals formed by this method have excellent size uniformity and position controllability. Structures consisting of metal nanocrystals in an extremely thin SiO<sub>2</sub> layer offer the possibility of developing new electronic devices such as high-temperature single electron tunnel diodes. A high throughput in fabricating nanoscale structures is another attractive feature offered by using this technique.

The authors thank Dr. Y. Tosaka for his helpful discussions and Dr. T. Ito for his encouragement.

<sup>1</sup>W. Chen, H. Ahmed, and K. Nakazato, *Appl. Phys. Lett.* **66**, 3383 (1995).

<sup>2</sup>F. Hache, D. Ricard, C. Flytzanis, and U. Kreibig, *Appl. Phys. A: Solids Surf.* **47**, 347 (1988).

<sup>3</sup>K. Becker, L. Yang, R. F. Haglund, Jr., R. H. Magruder, R. A. Weeks, and R. A. Zuhr, *Nucl. Instrum. Methods Phys. Res. B* **59 & 60**, 1304 (1991).

<sup>4</sup>K. Fukumi, A. Chayahara, K. Kadono, T. Sakaguchi, Y. Horino, M. Miya, J. Hayakawa, and M. Satou, *Jpn. J. Appl. Phys., Part 2* **30**, L742 (1991).

<sup>5</sup>H. Hosono, R. A. Weeks, H. Imagawa, and R. Zuhr, *J. Non-Cryst. Solids* **120**, 250 (1990).

<sup>6</sup>G. W. Arnold and J. A. Borders, *J. Appl. Phys.* **48**, 1488 (1977).

<sup>7</sup>L. C. Nistor, J. van Landuyt, J. D. Barton, D. E. Hole, N. D. Skelland, and P. D. Townsend, *J. Non-Cryst. Solids* **162**, 217 (1993).

<sup>8</sup>A. Perez, M. Trieilleux, T. Capra, and D. L. Griscom, *J. Mater. Res.* **2**, 910 (1987).

<sup>9</sup>A. Nakajima, H. Aoyama, and K. Kawamura, *Jpn. J. Appl. Phys., Part 2* **33**, L1796 (1994).

<sup>10</sup>F. J. Grunthaner, P. J. Grunthaner, R. P. Vasquez, B. F. Lewis, and J. Maserjian, *Phys. Rev. Lett.* **43**, 1683 (1979).

<sup>11</sup>H. Hosono, H. Fukushima, Y. Abe, R. A. Weeks, and R. A. Zuhr, *J. Non-Cryst. Solids* **143**, 157 (1992).